

On the Sample Complexity of Phase-Retrieval Receiver Based on 2-D Arrayed Photodetectors

Yuki Yoshida¹, Toshimasa Umezawa¹, Atsushi Kanno¹, Keizo Inagaki¹,
Naokatsu Yamamoto¹, and Tetsuya Kawanishi^{1,2}

¹National Institute of Information and Communications Technology, 4-2-1, Nukui-kitamachi, Koganei, Tokyo 184-8795, Japan

²Waseda University, 3-4-1 Ookubo, Shinjuku-ku, Tokyo 169-8555, Japan

¹yuki@nict.go.jp

Abstract: Sample complexity, or equivalently the required number of photodetectors, of a carrier-less phase-retrieving coherent receiver is investigated numerically based on the experimental data; it can achieve comparable complexity to conventional coherent receivers. © 2020 The Author(s)

1. Introduction

As a low-complexity coherent receiver solution for optical short-reach applications, a carrier-less coherent receiver based on phase retrieval (PR) has been demonstrated recently [1,2]. In the PR receiver, an optical phase-modulated signal is reconstructed from multiple magnitude-only measurements computationally based on PR, which has a rich history in many areas, including electron microscopy and crystallography [3]. No local light sources or optical hybrids are needed. As far as the authors know, two PR receiver architectures have been demonstrated experimentally so far. One is based on random sampling through diffraction [1] (Fig. 1). Another exploits a complementary measurement through a dispersive medium [2]. The latter approach allows to reconstruct an unknown from two intensity measurements. Meanwhile, as it relies on the random sampling, the former approach is spatially flexible and has potential to be a universal receiver solution for optical space division multiplexing (SDM) systems. However, the random approach requires more samples. For instance, 6 photodetectors (PDs) were needed per SDM channel in the demonstration in [1,4]. A question is, how many PDs are needed/enough for the PR receiver based on random sampling in practice? Theoretically, with generic random sampling, the answer is around 4, namely the $4\mathcal{M} - 4$ conjecture [5,6]. However, in practice, the sampling through a diffraction medium, namely scrambler, cannot be purely random and structured. The actual sample complexity of the PR receiver jointly depends on the structure, the type of the PR algorithm employed, and the transmitted signal format.

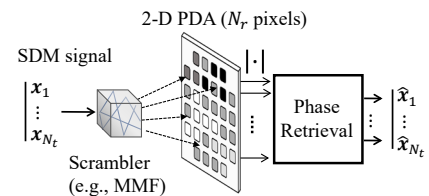


Fig. 1 PR-based coherent receiver [1].

In this work, we numerically investigate the sample complexity of the PR receiver by using a two-dimensional PD array (2-D PDA) proposed in [1,4]. Different PR algorithms are compared under practical assumptions. The results are further confirmed by numerical simulations based on the scrambler responses obtained experimentally.

2. Numerical Analysis

Suppose N_t -channel SDM signals are scrambled and detected by N_r arrayed PDs. We have the PR problem [4]:

$$\text{find } \mathbf{x} \quad \text{s.t.} \quad \mathbf{y} = |\mathbf{H}\mathbf{x}|, \quad (1)$$

where $\mathbf{x} \in \mathbb{C}^{N_t M \times 1}$ is a vector of the SDM signals, $\mathbf{y} \in \mathbb{R}_+^{N_r M \times 1}$ is a vector of magnitude-only measurements, $\mathbf{H} \in \mathbb{C}^{N_r M \times N_t M}$ represents the response of a scrambler, and M is a signal block size. Note that, $|\cdot|$ is defined as an element-wise operator here. One may solve (1) by minimizing the following amplitude-based loss function:

$$\min_{\mathbf{x}} l(\mathbf{x}) := \|\mathbf{y} - |\mathbf{H}\mathbf{x}|\|_2^2 / (2N_r M). \quad (2)$$

where $\|\cdot\|_2$ is the ℓ_2 -norm. In Table. 1, we summarize some low-complexity algorithms for the non-convex optimization in (2) suitable for high-speed communication applications. Due to the page limitation, we leave the technical detail of each algorithm to the literature. These algorithms guarantee the optimal sample and computational complexity orders in generic random sampling models [7-10]. From the practical point of view, their major differences are the computational burden for initialization and the sensitivity to the parameters. RAF and DRAF require a careful initialization and parameter tuning. The algorithms have comparable computational complexity per iteration, while PhareADMM needs a matrix inversion $(\mathbf{H}^H \mathbf{H})^{-1}$ in its initial step. In the simulation, we evaluated the algorithms in two different sampling models. The first model was a Gaussian random sampling model, i.e., $[\mathbf{H}]_{ij} \sim \mathcal{N}_c(0,1)$, as an ideal case. The second is a random convolutional sampling model for practical scramblers. In the second case, \mathbf{H} was given by a (block) Toeplitz matrix comprising of i.i.d. Rayleigh-fading channel response vector $\mathbf{h}_{ij} \sim \mathcal{N}_c(\mathbf{0}_{D \times 1}, \mathbf{I}_{D \times D})$ ($i = 1, \dots, N_r, j = 1, \dots, N_t$) where D denotes the channel memory length.

Table. 1 Low-complexity PR algorithms for amplitude-based loss function in (2). ($m := N_r M$ and $n := N_t M$)

Ref.	Computational complexity		Parameter sensitivity	Description
	per iteration	initialization		
RAF [7]	$O(mn)$	Spectral method ($O(mn)$)	High	A gradient descent-like approach based on the generalized gradient.
DRAF [4]	$O(mn)$	Spectral method	High	A robust RAF for discrete-valued signal reconstruction.
PhareADMM [8]	$O(mn)$	A matrix inversion is needed ($O(mn^2)$)	Low	Phases and amplitudes are separately updated based on the alternating direction method of multipliers (ADMM).
AMP.A [9]	$O(mn)$	Random initialization	Moderate	An approximate message passing (AMP) approach with ℓ_2 regularization.

Fig. 2 represents the bit-error rate (BER) performance versus the sample complexity $\Omega := N_r/N_t$. The BER is the averaged over 1000 realizations of \mathbf{H} in the absence of noise. \mathbf{H} is assumed to be known to the receiver. For fairness, each algorithm employed the weighted maximal correlation method [7] for initialization. The number of iterations was 600 for each case. We fixed $N_r = 16$ and $M = 64$, while N_t was adjusted depending on Ω . The QPSK format was employed. The parameters for RAF and DRAF were the same as in [4]. In the Gaussian sampling model in Fig. 2a), all the algorithms converged to the exact solution with high probability; the BERs were well below the 20%-FEC (forward error correction) threshold, i.e., $\text{BER} = 2.0 \times 10^{-2}$, for $\Omega > 4$. The conventional coherent receivers utilize 4 PDs (2 balanced-PDs) per channel. Therefore, the sample complexity of $\Omega = 4$ is comparable to that of the conventional receivers. However, the performance of the PR receiver was degraded in the practical convolutional model as in Fig. 2b). The structured PR problems are often ill-posed [10,11]. Especially, AMP.P did not converge in the model; RAF suffered from the error floor even without the noise. As in Fig. 2c) and d), the performance further deteriorated as the memory length D become shorter. In other words, the PR receiver requires a certain memory length for the scrambler. Even so, it was possible for DRAF and PhareADMM to achieve the FEC limit for $D=5$. Especially, PhareADMM achieved $\Omega = 3.2 (= 16/5)$ even with such ‘poor’ scrambler ($D=5$) at the expense of the computational cost in its initial step. Next, we investigate the noise tolerance of DRAF and PhareADMM. Fig. 2e) and f) show BER versus the number of iterations for different received SNR in the convolutional model with $D = 15$. Fig. 2e) and f) are for $\Omega = 4$ and 8, respectively. The SNR is defined in the optical domain, i.e., $\text{SNR} = E[\|\mathbf{H}\mathbf{x}\|_2^2]/E[\|\mathbf{n}\|_2^2]$ where $\mathbf{n} \in \mathbb{C}^{N_r M \times 1}$ denotes a noise vector. As shown in Fig. 2e), PhareADMM could achieve the comparable sample complexity to the conventional receivers for QPSK transmission if $\text{SNR} \geq 16$ dB. Meanwhile, the noise tolerance could be further improved by exploiting more samples as shown in Fig. 2f) ($\Omega = 8$). Particularly, the improvement, namely diversity gain, was significant in DRAF. In fact, the feature was a key to overcome the limited sensitivity of the prototype 2-D PDA in the proof-of-concept demonstration in [1,4] where $\Omega = 12$.

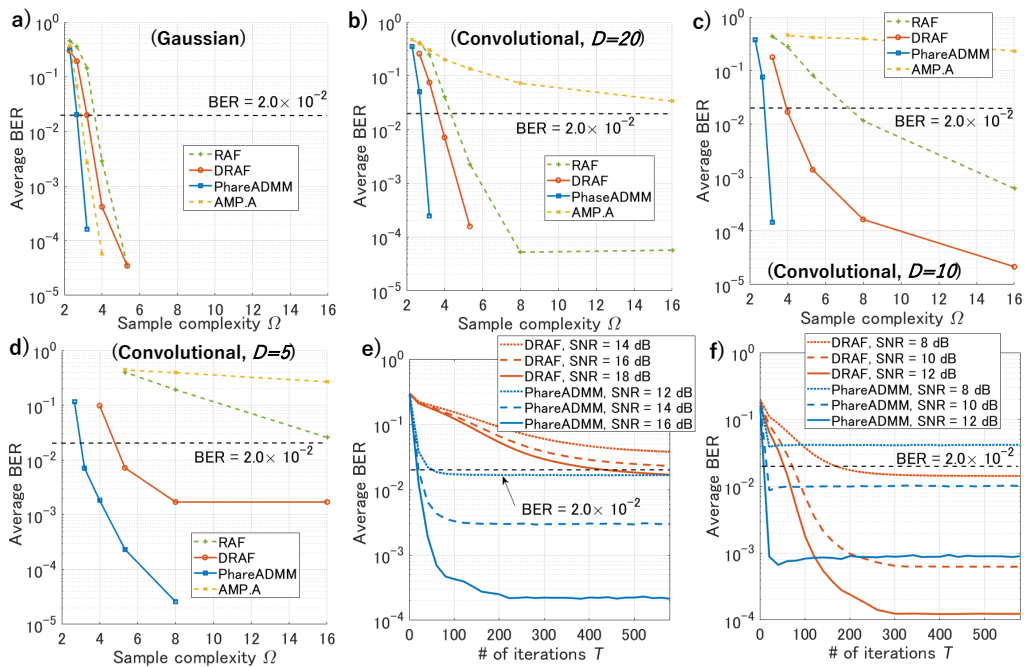


Fig. 2 Sample efficiency Ω versus BER for different measurement models: a) Gaussian random model, and random convolutional models with b) $D=20$, c) $D=10$, and d) $D=5$. Number of iterations T versus BER for e) $\Omega=4$ and f) $\Omega=8$ in the presence of noise.

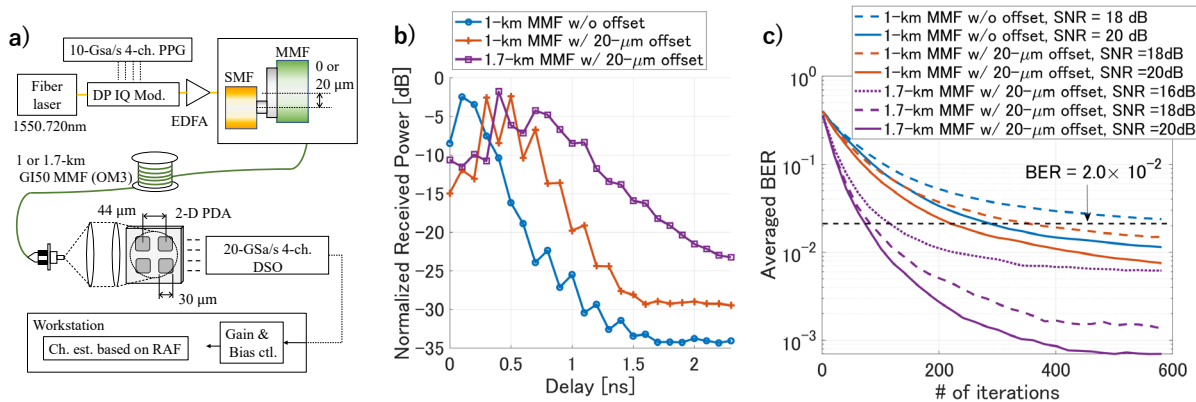


Fig. 3 a) Experimental setup, b) power delay profile of MMF-based scramblers, and c) BER versus number of iterations.

3. Numerical Simulation based on Experimental Data

We further investigate the achievable sample complexity of the PR receiver with PhareADMM numerically based on the response of the optical scramblers obtained experimentally. Fig. 3 a) is the experimental setup. At the transmitter, a < 0.1 -kHz-linewidth fiber laser output at 1550.72 nm was modulated by a dual-polarization (DP) optical IQ modulator driven by a 10-GSa/s pulse pattern generator (PPG) to generate a 10-Gbaud DP-QPSK signal, i.e., $N_t = 2$. The DP-QPSK signal was amplified to 17.5 dBm by an Erbium doped fiber amplifier (EDFA) and launched into an optical scrambler based on modal coupling and dispersion in a multimode fiber (MMF). We tested 1 and 1.7-km standard GI50 OM3 MMF with 0 and 20- μ m radial offset launching. The scrambler output was detected through collimate lens by a 4-pixel 2-D PDA (the central 4 PDs of the 32-pixel 2-D PDA [12]). The pixel size was 30 μ m \times 30 μ m with a 44- μ m pitch, and each pixel had 11-GHz bandwidth. The PD output was sampled by a 4-channel digital storage oscilloscope (DSO) at 20 GSa/s. The fractionally-spaced samples resulting from the 2-fold oversampling was exploited to increase the number of samples to 8 ($= 4 \times 2$) as in [1,4]. The resulting sample complexity was $\Omega = 8/2 = 4$. More specifically, the complexity was a half of the conventional receiver in sense of PD count and was the same with respect to ADC count. Based on 61,440 DP-QPSK symbols, the scrambler response \mathbf{H} including its phase was estimated via RAF in an offline manner (See [4] for the detail). For fairness, it should be mentioned that the SNR of the setup was not enough to reconstruct a DP-QPSK signal for $\Omega = 4$ due to the lack of the PD amplifiers. In fact, 12 PDs with 2-fold oversampling (i.e., $\Omega = 12$) were needed for DP-QPSK detection in [1,4]. However, it was possible to estimate the scrambler response with the aid of a long pilot sequence. The response \mathbf{H} was observed 100 times with slightly different fiber conditions to assess the statistical performance. of the PR receiver.

Fig. 3b) represents the averaged power delay profile of the estimated scrambler responses, i.e., $\sum_{i,j} |h_{ij}|^2$. Fig. 3c) shows the averaged BER performance evaluated numerically based on the scrambler responses in the presence of (simulated) noise. Although the 8 space-time channels were correlated each other unlike in the previous numerical simulations, it was possible to achieve the 20%-FEC limit via PhareADMM. With a 1-km MMF with and without 20- μ m offset launching, BER below the FEC limit was achieved for SNR > 18 dB and 20 dB, respectively. With a longer fiber of 1.7 km, the effective channel memory length $D \cong 10$ at 10 GSa/s, and DP-QPSK signals could be retrieved for SNR ≥ 16 dB with the sample complexity comparable to the conventional coherent receivers.

4. Conclusions

We investigated the sample complexity of a diffraction-based PR receiver by using a 2-D PDA. Numerical results based on the scrambler response obtained experimentally indicate that, for QPSK transmissions, the PR receiver with some practical scramblers has potential to achieve the comparable sample complexity to the conventional coherent receivers, i.e., 4 PDs (2 balanced-PDs) per channel and/or 2 ADCs per channel.

Acknowledgements: This work was partly supported by JSPS KAKENHI (Grant Numbers: JP19K04384), Japan.

5. References

- [1] Y. Yoshida *et al.*, OFC2019, Th4A.3 (2019).
- [2] H. Chen *et al.*, arXiv:1712.00716 (2019).
- [3] Y. Shechtman *et al.*, IEEE Signal Process. Mag. **32**(3), 87 (2015).
- [4] Y. Yoshida *et al.*, JLT, DOI: 10.1109/JLT.2019.2947305.
- [5] A. S. Bandeira *et al.*, Appl. Computat. Harm. Anal. **37**(1), 106 (2014).
- [6] A. Conca *et al.*, Appl. Comput. Harmon. Anal. **38**(2), 346 (2015).
- [7] G. Wang *et al.*, IEEE Trans. Signal Process. **66**(11), 2818 (2018).
- [8] J. Liang *et al.*, IEEE Signal Process. Lett. **25**(1), 5 (2018).
- [9] J. Ma *et al.*, IEEE Trans. Inf. Theory **65**(6), 3600 (2019).
- [10] M. Soltanolkotabi, IEEE Trans. Inf. Theory **65**(4), 2374 (2019).
- [11] Q. Qu *et al.*, arXiv:1712.00716, (2017).
- [12] T. Umezawa *et al.*, JLT **36**(7), 3684 (2018).